Journal of the Association of Arab Universities for Basic and Applied Sciences (2013) **13**, 19–23

University of Bahrain

Journal of the Association of Arab Universities for Basic and Applied Sciences

www.elsevier.com/locate/jaaubas
www.sciencedirect.com

تأثير فارق الرنين لدالــة طيف الموجات الصغيرة لنموذج ذرة تحت تأثير مجال نبضي

محمد رضا قادر

جامعة البحرين، كلية الهندسة، قسم الهندسة الكهربائية والمكانيكية

الملخص:

دراسة عددية وتحليل لطبيعة دالة طيف الموجات الصغيرة لذرة في وجود مجال ليزر نبضي ذات تردد مختلف عن تردد الذرة، وتحليل ودراسة متغيرات النموذج مع فارق الرنين. أظهرت الحسابات العددية لدالة الطيف على أن دالة الطيف لها سلوك غير متماثل وذلك بسبب وجود فارق الرنين، بارمتر فارق الإزاحة، أياً كان شدة المجال النبضي والدالة تكون غير متماثلة أكثر مع بارمتر الإزاحة.

Journal of the Association of Arab Universities for Basic and Applied Sciences (2013) **13**, 19–23

University of Bahrain

Journal of the Association of Arab Universities for Basic and Applied Sciences

www.elsevier.com/locate/jaaubas
www.sciencedirect.com

ORIGINAL ARTICLE

Detuning effects in Haar wavelet spectrum of pulsed-driven qubit

M.R. Qader

University of Bahrain, Department of Electrical and Electronics Engineering, Bahrain

Available online 29 November 2012

KEYWORDS

Haar wavelet;
Driven qubit;
Radiation;
Laser pulse

Abstract The transient scattered radiation due to interaction of a short laser pulse (of rectangular shape) with a qubit is studied through the Haar wavelet window spectrum. Asymmetrical structure in the spectrum is shown due to frequency miss-match of the laser and qubit frequencies and the shift window parameter.

1. Introduction

Analyzing the scattered radiation due to the interaction of a single qubit (taken as spin-$\frac{1}{2}$ or 2-level atom system) with a short laser pulse is one of the many basic studies in signal information processing. Within a quantum framework the (transient) scattered radiation, known as fluorescent spectrum, is quantified as the Fourier transform (FT) of the auto-correlation function of the induced atomic dipoles (Mollow, 1969; Eberly and Wodkiewicz, 1977; Eberly, 1984). Transient florescent spectra of 2-level atomic systems (qubits) driven by different shapes of laser pulses (e.g., rectangular, triangular, etc. Newbold and Saloma, 1980; Rzazewski and Florjanczyk, 1984; Florjanczyk et al., 1985; Haus et al., 1984; Rodgers and Swain, 1991; Joshi and Hassan, 2002; Hassan et al., 2008, 2010) have been studied in detail.

In the usual Fourier analysis, a signal is represented as sum of sinusoidal functions of various frequencies. This is suitable for signals that change very slowly with time or for very noisy signals that change regularly with time (David, 2000; Addison, 2004). For non-stationary signals and signals with sudden change, Fourier analysis averaging over the entire length of the signal and hence the fixed time-width windowed FT has its limitation, as some "fine" detail is lost. Such "fine detail" or time localization analysis of different frequency components of a given signal is called wavelet transform (Croca, 2003). With windowed wavelet transform, the time width is adjusted to the frequency in such a way that high frequency wavelets will be narrow and vice-versa (Feruandez and Rojas, 2002). For resonant rectangular pulsed-driven qubit models, wavelet transform of the scattered radiation has been examined with different window functions: Morlet's and Mexican hat wavelets (Mohamed et al., 2007) and Haar wavelet (Hassan et al., 2011).

In the present work, we examine the transient fluorescent Haar wavelet spectrum of a single qubit excited by a non-resonant rectangular laser pulse and compare the results with the corresponding ones for the resonant case (Hassan et al., 2011). The paper is presented as follows in Section 2, we present the essential analytical formulas for the Haar wavelet spectrum, followed by discussion of computational plots in Section 3. A summary is given in Section 4.

2. Haar wavelet transient spectrum

For a single qubit excited by a short laser pulse, the general form of the transient scattered radiation is given by (Eberly and Wodkiewicz, 1977; Rodgers and Swain, 1991).

E-mail address: mrqader@eng.uob.bh

Peer review under responsibility of University of Bahrain.

ELSEVIER Production and hosting by Elsevier

1815-3852
http://dx.doi.org/10.1016/j.jaubas.2012.09.001

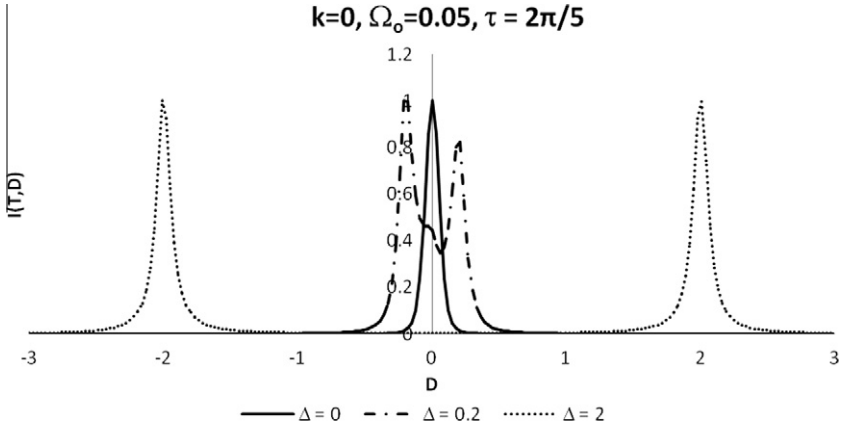

Figure 1a Transient Haar wavelet normalized spectrum $I(\tau, D)$ verses the filter's detuning parameter D for $\Omega_0 = 0.05$, $\tau = 2\pi/5$, $k = 0$ and various values of atomic detuning $\Delta = 0,0.2,2$.

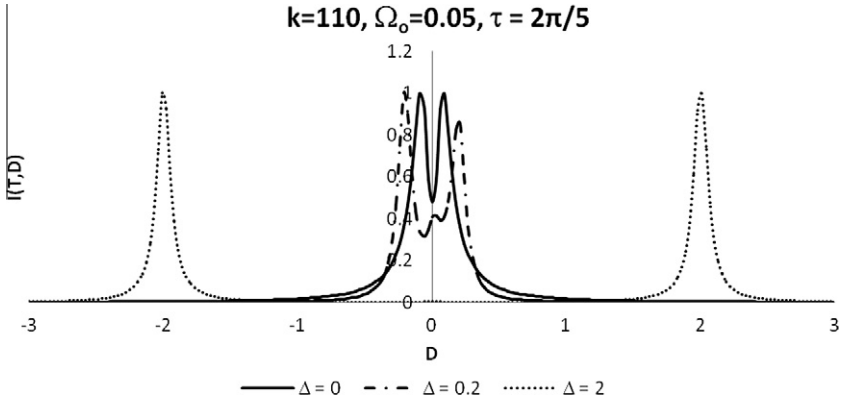

Figure 1b As Fig. 1a but for $k = 110$.

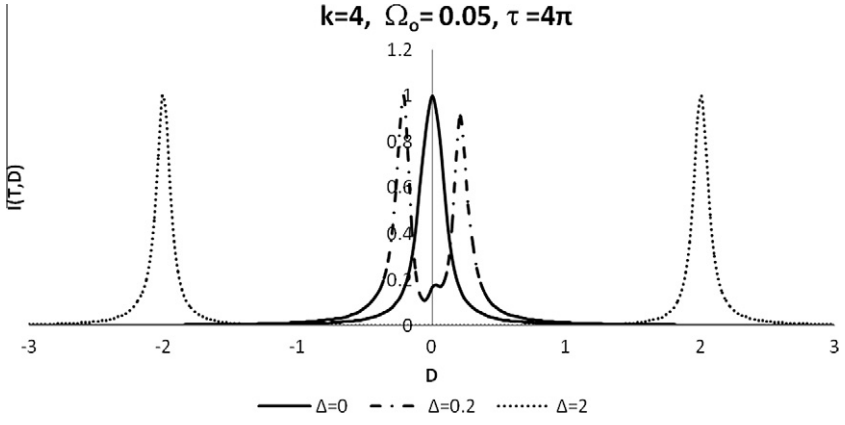

Figure 1c As Fig. 1a but for $k = 4$, $\tau = 4\pi$.

$$S(t,\omega_f,\Gamma) = 2\Gamma \int_{-\infty}^{t} dt_1 \int_{-\infty}^{t} dt_2 H(t-t_1)H^*(t-t_2) \times \langle \widehat{S}_+(t_1)\widehat{S}_-(t_2)\rangle \quad (1)$$

Where $\widehat{S}_+(t_1)\widehat{S}_-(t_2)$ is the quantum average of the atomic dipole–dipole spin auto-correlation function with $\widehat{S}_\pm$ are the atomic spin-up (down) operators and $H(t)$ is the (filter) window function of the radiation detector. For the case of narrow Lorentzian filter, it has the form

$$H_F(t) = e^{i\omega_f t} e^{-\Gamma|t|} \quad (2)$$

Where ω_f and Γ are the central frequency and width of the filter, respectively. With the narrow window function (2) the

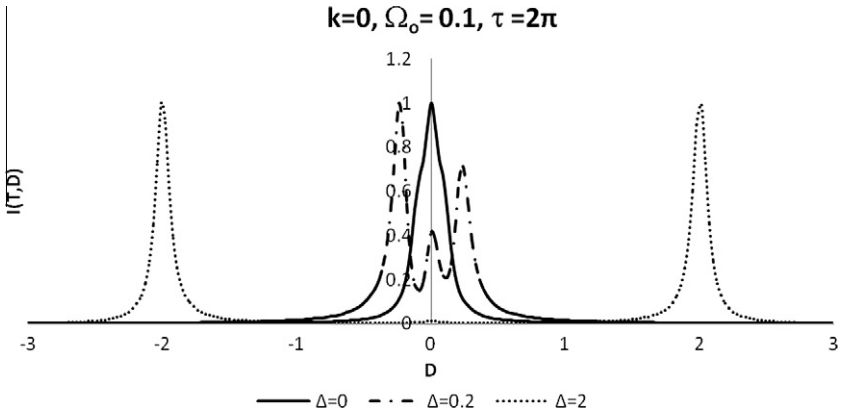

Figure 2a As Fig. 1a but for $\Omega_0 = 0.1$, $\tau = 2\pi$.

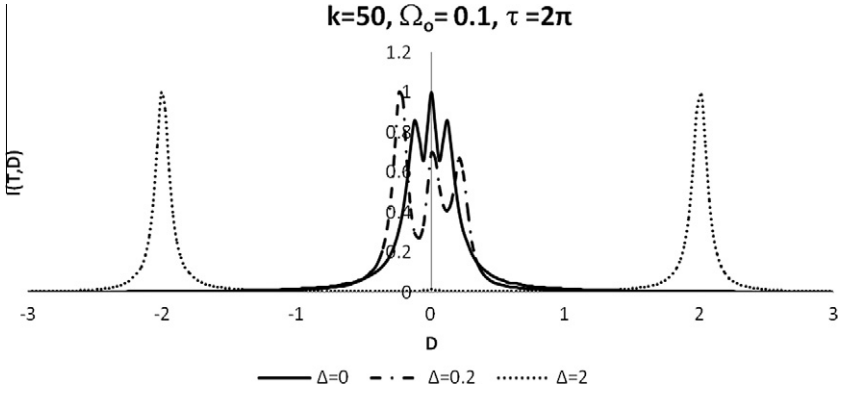

Figure 2b As Fig. 1a but for $\Omega_0 = 0.1$, $\tau = 2\pi$, $k = 50$.

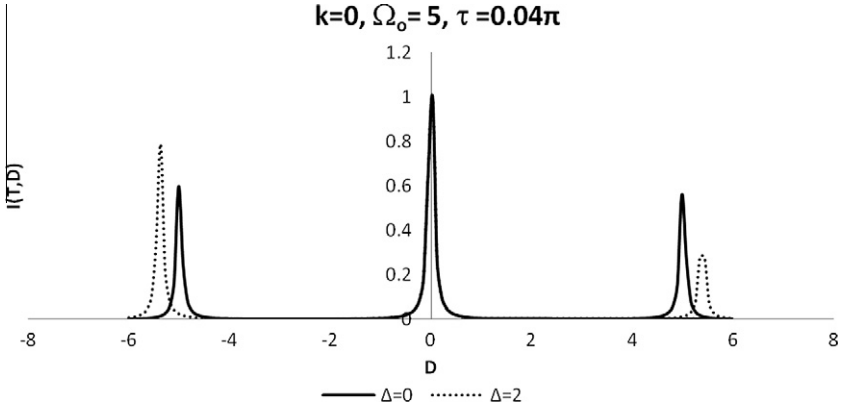

Figure 3a As Fig. 1a but for $\Omega_0 = 5$, $\tau = \pi/25$, $k = 0$, $\Delta = 0,2$.

filter "sees" the detected field in the Fourier domain (Eberly, 1984). The investigation of the current model for the transient FT spectrum (i.e., (1) with (2)) is given in (Rodgers and Swain, 1991; Joshi and Hassan, 2002). Now, in the present case, the Haar wavelet window function $H_h(t)$ is given by (Rodgers and Swain, 1991, references therein),

$$H_h(t - t_1) = \Psi(t - t_1)e^{(i\omega_f - \Gamma)(t - t_1)} \tag{3}$$

Where the Ψ(t) is the mother wavelet function,

$$\Psi(t - t_1) = 2^{\frac{j}{2}} \begin{cases} -1, & a \leqslant t_1 < b \\ 1, & b \leqslant t_2 < c \\ 0, & \text{otherwise} \end{cases} \tag{4a}$$

Where $a < b < c$, are given by,

$$\begin{aligned} a &= t - (1 + k)(2)^{-j} \\ b &= t - \left(\frac{1}{2} + k\right)(2)^{-j} \\ c &= t - (k)(2)^{-j} \end{aligned} \tag{4b}$$

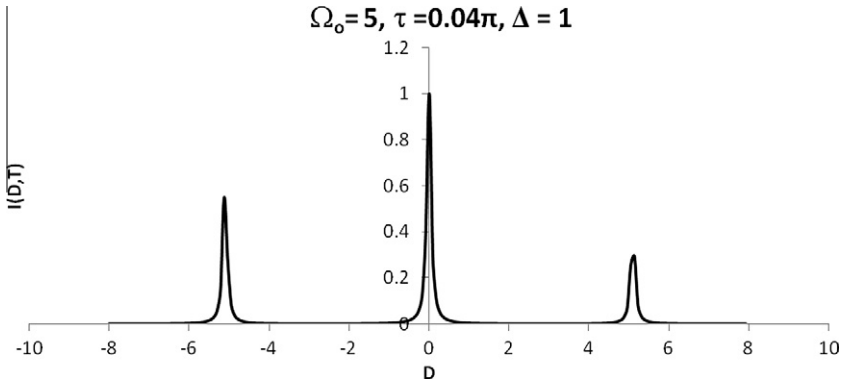

Figure 3b As Fig. 3a but at fixed $\Delta = 1$ ($k \geqslant 0$ gives the same figure).

With j and k are the dilation and shift parameters respectively. The filler's frequency (ω_f) and width (Γ) parameters have been introduced via the exponential factor in (3). For a short laser pulse the interaction with the qubit takes place in the absence of any damping process. In the case of a rectangular laser pulse, the expression for the dipole auto-correlation function for initially ground state atom is given by (Hassan et al., 2008),

$$\langle \widehat{S}_+(t_1)\widehat{S}_-(t_2)\rangle = e^{i\omega_a(t-t_1)}\left[C_-(t_1)C_-^*(t_1) + \frac{1}{4}C_z(t_1)C_z^*(t_2)\right] \quad (5)$$

With the C-number functions $C_{-,z}(t)$ are given by

$$C_-(t) = \frac{1}{2}\left(\frac{\Omega_o}{\Omega_1}\right)^2 (1 - cos\Omega_1 t)$$
$$C_z(t) = \frac{\Delta\Omega_o}{\Omega_1^2}(1 - cos\Omega_1 t) - i\frac{\Omega_o}{\Omega_1}\sin\Omega_1 t \quad (6)$$

Where $\Omega_1 = \sqrt{\Omega_o^2 + \Delta^2}$, Ω_o is the (real) Rabi frequency associated with the laser pulse and $\Delta = (\omega_a - \omega_L)$ is the frequency detuning between the atomic transition frequency (ω_a) and the circular frequency (ω_L) of the laser pulse.

Inserting the expression (2–6) into the formula (1), we have the Haar wavelet transient spectrum at the end of pulse duration, $t = T$ in the form,

$$S(T, D, \Gamma) = \frac{\Gamma}{2}e^{-2\Gamma T}(|J_1(T)|^2 + |J_2(T)|^2) \quad (7)$$

$$J_1(T) = -(2)^{\frac{j}{2}}\left[\int_a^b - \int_b^c\right]e^{(\Gamma+iD)t'}C_-(t')dt'$$
$$= (2)^{\frac{j}{2}}(1 - 2e^{-2^{-j-1}} + e^{-2^{-j}})\left(\frac{\Omega_o}{\Omega_1}\right)^2\left[\frac{e^{(\Gamma+iD)(T-2^{-j}k)}}{\Gamma + iD}\right.$$
$$\left.+\left\{-\frac{1}{2}\frac{e^{(\Gamma+i(D-\Omega_1)(T-2^{-j}k)}}{\Gamma + i(D-\Omega_1)} + (\Omega_1 \to -\Omega_1)\right\}\right] \quad (8a)$$

$$J_2(T) = -(2)^{\frac{j}{2}}\left[\int_a^b - \int_b^c\right]e^{(\Gamma+iD)t'}C_z(t')dt'$$
$$= (2)^{\frac{j}{2}-1}(1 - 2e^{-2^{-j-1}} + e^{-2^{-j}})\left(\frac{\Omega_o}{\Omega_1}\right)\left\{\left[\frac{e^{(\Gamma+iD)(T-2^{-j}k)}}{\Gamma + iD} - (\Omega_1 \to -\Omega_1)\right]\right.$$
$$\left.+\left(\frac{\Delta}{\Omega_1}\right)J_1(T)\right\} \quad (8b)$$

With $D = \omega_L - \omega_f$ is the filter's detuning parameter. Note that, the parameter ($2^{-j}k$) can be considered as an effective shift parameter. At exact resonance $\Delta = 0$ the expressions (8) reduce to those in (Hassan et al., 2011).

3. Discussion of results

Here, we present the plotting of the normalized spectrum $I(T,D) = S(T,D)/S_{max}(T,D)$ in Figs. (1–3) after normalizing the parameters Ω_o,D, by (Γ). We use the same data in (Hassan et al., 2011) in order to see the effect of the atomic detuning on the structure of the spectrum.

For weak pulse strength $\Omega_o = 0.05$ and $\tau = T - 2^{-j}k = 2\pi/5, k = 0$ the single narrowed Lorentzian at $D = 0$ (Hassan et al., 2011) turns to asymmetrical splitting for small atomic detuning, $\Delta = 0.2$ (Fig. 1a), with asymmetry reversed for $\Delta = -0.2$. For larger $\Delta = 2$ the spectrum turns to two separate peaks (almost symmetrical) at $D = \pm 2$. For a larger shift parameter $k = 110$ where the dip structure at $D = 0$ (Hassan et al., 2011) shows reversed asymmetry compared with Fig. 1b and turns to separate peaks for increasing D (Fig. 1c). For larger $\tau = 4\pi, k = 4$ (Fig. 1c), the asymmetry of splitted peaks with small $\Delta = 0.2$ is reduced compared with Fig. 1a.

For relatively larger $\Omega_o = 0.1$, $\tau = 2\pi$, the 'pencil' shaped Lorentzian at resonance $\Delta = D = 0$ (Hassan et al., 2011) for $k = 0$ splits to 3-unequal peaks with small $\Delta = 0.2$ (Fig. 2a). With larger $k = 50$, the same splitting feature occurs for the "top" 3-peak structure for $\Delta = 0$ (Hassan et al., 2011) – (Fig. 2b).

For strong pulse strength $\Omega_o = 5$, $\tau = \pi/4$, $k = 0$ the symmetrical 3-peak Mollow structure gets asymmetrical for $\Delta \neq 0$ (Fig. 3a). At fixed $\Delta = 1$, the asymmetrical 3-peak structure is unaffected by the shift parameter k (Fig. 3b), unlike the weak pulse case.

4. Summary

For rectangular pulsed-driven qubit, initially in its ground state the Haar wavelet spectrum is symmetric at exact atomic resonance $\Delta = 0$, for arbitrary values of pulse strength (Ω_o) shift parameter (k), and the effective time parameter (τ) (Hassan et al., 2011). The effect of non-zero atomic detuning ($\Delta \neq 0$) is as follows:

1. For a weak pulse and $k = 0$, asymmetry is more pronounced for small $|\Delta| < 1$ and it is reversed with larger shift parameter (k). For larger $|\Delta| = 2$ aibitrary k,τ the spectrum splits into two symmetrical peaks at $|D| = 2$.
2. For a strong pulse, asymmetry shows in the two-side bands of the Mollow spectrum for $\Delta \neq 0$ and $k \geqslant 0$.

Finally we add that, for other initial atomic state preparation (e.g., coherent state) the Fourier spectrum at EXACT atomic resonance shows pronounced asymmetry on its profile due to the Rabi oscillations and their interference, which is caused by the initial coherent dispersion of the atomic polarization . Due to the lengthy analytical expressions for an initial atomic coherent state with non-zero atomic detuning, the results will be analysed with computational display in a separate presentation.

Acknowledgements

The author acknowledges the support of the University of Bahrain, research project (No. 2011/32). The author also acknowledges fruitful discussion with Prof. S.S. Hassan (University of Bahrain).

References

Addison, P., 2004. Physics world, (March issue) pp. 35–39.
Croca, J.R., 2003. Towards a Nonlinear Quantum Physics. World Scientific, London.
David, W.K., 2000. A First Course in Fourier analysis. Prentice Hall, NY.
Eberly, J.H., Wodkiewicz, K., 1977. J. Opt. Soc. Am. 67, 1252.
Eberly, J.H., 1984. In: Barut, A.O. (Ed.), Quantum Electrodynamics and Quantum Optics. Academic Press, NY, pp. 209–227.
Feruandez, R.M.C., Rojas, H.N.D., 2002. An overview of wavelet transforms application in power system. In: Proc. of 14th PSCC, Sevilla (June 24–28).
Florjanczyk, J., Rzazewski, K., Zakerzewski, J., 1985. Phys. Rev. A 31, 1558.
Hassan, S.S., Joshi, A., Al-Madahari, M.M., 2008. J. Phys. B 41, 145503, Corrigendum (2009) J. Phys. B. 42, 089801.
Hassan, S.S., Joshi, A., Batarfi, H.A., 2010. Int. J. Theor. Phys., Group Theor. Nonlinear Opt. 13, 371.
Hassan, S.S., Al-Saegh, M.A., Mohamed, A.A.S., Batarfi, H.A., 2011. Nonlinear Opt., Quantum Opt. 42, 37–50.
Haus, J.W., Lewenstein, M., Rzazewski, K., 1984. J. Opt. Soc. Am. B, 1641.
Joshi, A., Hassan, S.S., 2002. J. Phys. B 35, 1985.
Mohamed, A.A.S., Hassan, S.S., Al-Saegh, M.A., 2007. Nonlinear Opt., Quantum Opt. 36, 107–116.
Mollow, B.R., 1969. Phys. Rev. 188, 1969.
Newbold, M.A., Saloma, G.J., 1980. Phys. Rev. A 22, 2098.
Rodgers, P.A., Swain, S., 1991. Opt. Commun. 81, 291.
Rzazewski, K., Florjanczyk, M., 1984. J. Phys. B: At., Mol. Phys. 17, L509.